



Dihydrotanshinone I attenuates cisplatin-induced acute kidney injury by targeting TRIM28-mediated oxidative stress and apoptosis: insights from activity-based protein profiling and omics integration

Ping-Ping Sun, Jun-Yong Sun, Ze-Hua Li, Jing Chang, Mei-Ling Jin, Jia-Yu Song* , Qian-Mei Sun*, Xiao-Juan Wang*

Received: 27 March 2025 / Revised: 6 August 2025 / Accepted: 6 August 2025
© Youke Publishing Co., Ltd. 2025

Abstract Cisplatin, a platinum-based chemotherapeutic agent, is widely used in cancer treatment, but its limitation lies in its nephrotoxicity, which compromises its clinical use. This study investigated the therapeutic potential of dihydrotanshinone I (DHT), a natural diterpene from *Salvia miltiorrhiza*, in mitigating cisplatin-induced nephrotoxicity via dual antioxidant and antiapoptotic mechanisms. Using activity-based protein profiling, we identified tripartite motif containing 28 (TRIM28) as a direct molecular target of DHT in human proximal tubule epithelial cells. DHT treatment significantly attenuated cisplatin-induced cytotoxicity through TRIM28-mediated reduction of reactive oxygen species (ROS) accumulation and inhibition of apoptotic signaling. Proteomic analysis revealed that DHT restored cisplatin-altered protein expression linked to

oxidative stress and apoptosis pathways. Pretreatment with DHT (15 mg kg⁻¹ day⁻¹, oral gavage) in cisplatin-treated C57BL/6 mice preserved the renal function, reduced the acute tubular injury, and reversed the cisplatin-induced oxidative imbalance (enhanced superoxide dismutase activity, reduced malondialdehyde and ROS) and apoptotic signaling (BAX/Bcl-2, c-caspase 3) via in vivo experiments. These findings suggest that DHT is a promising renoprotective adjuvant for platinum-based chemotherapy.

Keywords Dihydrotanshinone I; Cisplatin nephrotoxicity; Tripartite motif containing 28; Oxidative stress; Apoptosis; Renal protection

1 Introduction

Cisplatin, a platinum-based chemotherapeutic agent, is extensively used for treating solid tumors such as ovarian, lung, and bladder cancers [1–3]. However, its clinical use is restricted by dose-dependent nephrotoxicity, which manifests in 30% of patients and often necessitates dose reduction or treatment discontinuation [4–7]. The pathophysiology of cisplatin-induced acute kidney injury (AKI) is multifactorial and involves oxidative stress, DNA damage, mitochondrial dysfunction, and inflammatory responses [8–11]. Recent studies have highlighted that cisplatin disrupts the redox balance by generating excessive reactive oxygen species (ROS) [12–15]. Despite advancements in hydration protocols and antioxidant adjuvants (e.g., N-acetylcysteine (NAC)), effective strategies for alleviating cisplatin nephrotoxicity are lacking [16–20].

Natural compounds have garnered attention for their multitargeted biological activities, particularly in reducing oxidative stress and inflammation [21–27]. *Salvia*

P.-P. Sun, J. Chang, X.-J. Wang*
Department of Internal Medicine, Beijing Chao-Yang Hospital,
Capital Medical University, Beijing 100020, China
e-mail: xjwang730715@sina.com

J.-Y. Sun
Department of Radiology, Shandong Cancer Hospital and
Institute, Shandong First Medical University and Shandong
Academy of Medical Science, Jinan 250117, China

Z.-H. Li
Renal Division, Peking University Institute of Nephrology,
Peking University First Hospital, Beijing 100034, China

M.-L. Jin, Q.-M. Sun*
Department of Nephrology, Beijing Chao-Yang Hospital,
Capital Medical University, Beijing 100020, China
e-mail: sunqianmei5825@163.com

J.-Y. Song*
Department of Pediatric Nephrology, The Second Affiliated
Hospital of Nanjing Medical University, Jiangsu 210003, China
e-mail: songjiayu@njmu.edu.cn



multiorrhiza (Danshen), a key traditional Chinese medicinal herb, has served as a therapeutic agent throughout Chinese history as a treatment for cardiovascular and cerebrovascular disorders. Dihydrotanshinone I (DHT), a bioactive diterpene derived from *S. multiorrhiza*, exhibits antioxidative, anti-inflammatory, and anticancer properties [28–34]. Its lipophilic nature enables efficient cellular uptake, and recent evidence suggests that it has the potential to attenuate organ damage (e.g., kidney, liver, and heart) induced by chemotherapeutic agents [35, 36]. Nevertheless, the molecular mechanisms underlying DHT's renoprotective effects have not been fully elucidated.

This study integrates activity-based protein profiling (ABPP) and proteomic, biochemical, and pharmacological approaches to establish how DHT ameliorates cisplatin nephrotoxicity. We demonstrated that DHT protects renal tubular epithelial cells by targeting TRIM28, an E3 ubiquitin ligase that restores proteomic equilibrium, alleviates oxidative stress, and inhibits apoptosis. These insights provide a foundation for establishing DHT as a safe and effective adjuvant in platinum-based therapies.

2 Experimental

2.1 Cell experiments

2.1.1 Cell culture and treatments

Human renal proximal tubular epithelial cells (HK2, ATCC® CRL-2190™) were maintained in Dulbecco's modified Eagle medium (Gibco, 12491015) supplemented with 10% fetal bovine serum (Gibco, A5670201) and 1% penicillin–streptomycin (Beyotime, C0224) at 37 °C under 5% CO₂ conditions. For drug treatments, cells were pre-treated with DHT (MedChemExpress, HY-N0360) at concentrations of 50, 100, 150, and 200 μM for 2 h, followed by exposure to 10 μM cisplatin (Sigma, P4394) for 24 h. The control groups received equivalent volumes of dimethyl sulfoxide (DMSO; Sigma, D2650; final concentration < 0.1%). In the functional validation experiments, 2 mM NAC (Sigma, A9165) or 20 μM Z-VAD-FMK (Selleck, S7023) was co-administered with cisplatin.

2.1.2 Competitive in-gel fluorescent labeling assay

HK2 cells (1×10^6 cells well⁻¹) were seeded in 6-cm culture dishes and incubated with DHT (0, 20, 40, or 80 μM). After 4 h, the cells were harvested and lysed. Total protein concentrations were quantified using a BCA assay. The lysates were labeled with a cysteine-specific iodoacetamide probe (IAA-probe) at 37 °C with gentle agitation for 1 h. Subsequent click chemistry reactions

were performed by adding azide-TAMRA (100 μM), CuSO₄ (500 μM), TBTA (50 μM), and TCEP (500 μM). Proteins were separated by 12% SDS-PAGE (Bio-Rad, P0919S), and in-gel fluorescence signals were visualized using an Azure Sapphire RGB NIR scanner. Coomassie Brilliant Blue staining confirmed equal protein loading across the lanes.

2.1.3 ABPP

Competitive ABPP was performed as previously described [37] with modifications. Briefly, HK2 cell lysates were pre-incubated with DHT or DMSO for 1 h at 4 °C, followed by labeling with an IAA-alkyne probe (Click Chemistry Tools, 1067) for 1 h at 37 °C. Click chemistry reactions were performed using a TAMRA-azide conjugate (Click Chemistry Tools, 1348) under Cu(I)-catalyzed conditions. Labeled proteins were resolved by 12% SDS-PAGE and visualized using an Azure Sapphire RGB NIR scanner. For target identification, gel bands exhibiting reduced fluorescence were excised, digested with trypsin, and analyzed by LC–MS/MS (Thermo Fisher Scientific, Orbitrap Fusion Lumos, USA).

2.1.4 Fluorescence colocalization assay

Immunofluorescence imaging was performed to assess colocalization between the IAA-probe and TRIM28. After probe competition and click reactions, the cells were processed as follows: (1) overnight incubation with rabbit anti-TRIM28 (Proteintech 15202–1-AP, 1:300) in blocking buffer at 4 °C; (2) three washes with TBST (5 min each), followed by incubation with a fluorescence-labeled secondary antibody (goat anti-rabbit IgG, Bioss, 1:1000) at room temperature in the dark for 2 h; (3) nuclear counterstaining with Hoechst 33,342 (1:1000, 30 min), followed by three washes with TBST; (4) mounting with 90% glycerol and imaging via confocal microscopy (Leica TCS SP8 SR). Colocalization was calculated using Pearson's coefficient (ZEN 3.4), and changes in fluorescence intensity were quantified by competition (DHT vs. IAA-probe) and target engagement (IAA-probe/TRIM28).

2.1.5 Pull-down assay

To confirm the direct interaction between DHT and TRIM28, a pull-down assay was performed coupled with western blotting. After click chemistry reactions, the samples were denatured with 1 × loading buffer at 90 °C for 10 min. The enriched proteins were resolved via 12% SDS-PAGE and transferred to polyvinylidene fluoride membranes. Immunoblotting utilized a rabbit anti-TRIM28 antibody (Proteintech 15202–1-AP, 1:1000) followed by HRP-conjugated secondary antibodies (CST, 1:5000).

Signals were detected using an ECL substrate (Bio-Rad) and quantified via ImageLabTM software.

2.1.6 ROS detection

Intracellular ROS levels were measured using the fluorescent probe 2',7'-dichlorodihydrofluorescein diacetate (DCFH-DA; Beyotime, S0033S). Briefly, cells were incubated with 10 μ M DCFH-DA in serum-free medium for 30 min at 37 °C, followed by three washes with PBS. Fluorescence images were captured using a confocal microscope.

2.1.7 Apoptosis analysis

Apoptosis was quantified via Annexin V-FITC/PI double staining using the Annexin V-FITC Apoptosis Detection Kit (BD, 556547). Cells were analyzed by flow cytometry (BD LSRFortessaTM), and data were processed using FlowJo v10.8.1.

2.1.8 Molecular docking

The 3D structure of DHT was retrieved from the SciFinder database, while the crystal structure of TRIM28 (PDB ID: 8CR0) was downloaded from the RCSB PDB database. Protein preparation, including dehydration and hydrogenation, was performed using AutoDock Tools (v1.5.6). Furthermore, molecular docking simulations were conducted with AutoDock Vina (v1.2.3), and PyMOL (v2.5.2) was used for structural visualization and binding interaction analysis.

2.1.9 Differential expression and functional enrichment analysis

Differentially expressed genes were identified from RNA-Seq data using the $\log_2(\text{fold change}) > 1$ and adjusted $p < 0.05$ thresholds, with results visualized via volcano plots (ggplot2, v3.4.2). The KEGG pathway and Gene Ontology (GO, comprising the biological process, cellular component, and molecular function categories) enrichment analyses were performed using clusterProfiler (v4.8.1) with significance thresholds of $p < 0.05$ and false discovery rate (FDR) < 0.1 . Functional interaction networks were reconstructed using the STRING database (v12.0; interaction score > 0.7), refined in Cytoscape (v3.9.1; topology filtering, MCODE scoring ≥ 4), and validated against published literature.

2.2 Animal experiments

Male C57BL/6 mice (8 weeks old, 20–25 g) were procured from Beijing Vital River Laboratory Animal Technology Co., Ltd. and housed under standard conditions (12-h

light/dark cycle, 22 °C) with ad libitum access to water and a standard diet. All animal procedures were reviewed and approved by the Ethics Committee of Capital Medical University (approval number AEEI-2022-200).

Mice were randomly divided into control (CON), cisplatin (CIS, 20 mg kg⁻¹ single dose), and DHT treatment (15 mg kg⁻¹ day⁻¹ via oral gavage for 7 days, followed by cisplatin administration) groups. Blood and kidney tissue samples were collected 72-h post-cisplatin administration. Serum creatinine (CREA) and blood urea nitrogen (BUN) levels were measured using commercial ELISA kits (Jiancheng Bioengineering, C011-2-1 and C013-2-1). Kidney tissues were stained with hematoxylin and eosin (H&E) for tubular injury scoring (necrosis, brush border loss, and casts), western blot analysis (cleaved caspase 3, BAX, Bcl-2, and KIM-1), and oxidative stress marker detection (superoxide dismutase (SOD), malondialdehyde (MDA), and ROS) using commercial kits.

2.3 Statistical analysis

Experimental data are presented as mean \pm standard deviation/standard error of mean (mean \pm SD/SEM), and statistical analyses were performed using SPSS 22 and GraphPad Prism 9.0 software. Comparisons were evaluated using the Student's t-test and analysis of variance (ANOVA), with statistical significance defined as $*p < 0.05$, $**p < 0.01$, $***p < 0.001$, and $****p < 0.0001$.

3 Results and discussion

3.1 DHT protects HK2 cells against cisplatin-induced cytotoxicity and suppresses apoptosis in vitro

Figure 1A shows the chemical structure of DHT. To investigate the protective effects of DHT against cisplatin-induced cytotoxicity, we evaluated the viability of HK2 cells treated with increasing concentrations of DHT (50–200 μ M) in the presence or absence of cisplatin (10 μ M). HK2 cell viability was significantly reduced in the CIS group compared with the control group ($38.4\% \pm 3.2\%$ vs. $100\% \pm 1.4\%$, $****p < 0.0001$) (Fig. 1B). However, DHT treatment improved cell viability in a dose-dependent manner, with a maximum effect observed at 200 μ M ($83.4\% \pm 2.8\%$, $****p < 0.0001$ vs. CIS alone).

We further examined the ability of DHT to mitigate cisplatin-induced oxidative stress by measuring the intracellular ROS levels via flow cytometry. Cisplatin-treated cells

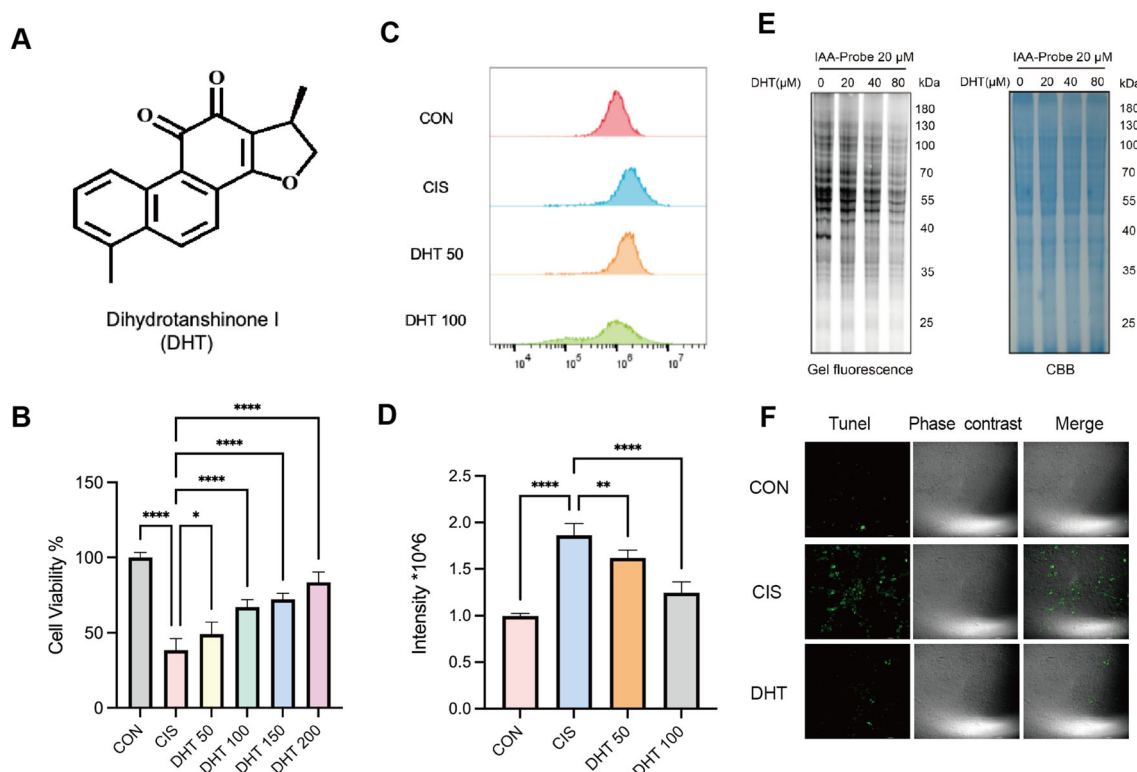


Fig. 1 Evaluation of DHT efficacy. **A** Chemical structure of dihydrotanshinone I (DHT). **B** Detection of cell viability of HK2 cells treated with cisplatin and different concentrations of DHT for 24 h. **C** Flow cytometry histograms showing the intracellular reactive oxygen species (ROS) levels in HK2 cells under different conditions. **D** Quantification of ROS fluorescence intensity based on flow cytometric data. **E** DHT competed with the iodoacetamide (IAA)-alkynyl probe for binding to the protein cysteine residues in HK2 cells. Left, in-gel fluorescence. Right, Coomassie Brilliant Blue (CBB) staining. **F** TUNEL staining demonstrated that DHT treatment significantly mitigated cisplatin-induced apoptosis. * $p < 0.05$, ** $p < 0.01$, *** $p < 0.001$, **** $p < 0.0001$

exhibited markedly increased ROS generation ($(1.86 \pm 0.06) \times 10^6$, $(0.99 \pm 0.01) \times 10^6$, **** $p < 0.0001$) compared to the control group, while 100 μM DHT significantly reduced ROS fluorescence intensity ($(1.25 \pm 0.06) \times 10^6$, ** $p < 0.01$ vs. CIS alone) (Fig. 1C, D).

Moreover, the in-gel fluorescence assay based on ABPP showed that DHT competes with the IAA-alkyne probe for labeling protein fluorescence, thus demonstrating that DHT binds covalently to the target protein cysteine residues in HK2 cells (Fig. 1E). The TUNEL assay revealed severe apoptosis in the CIS group, as evidenced by the increased green fluorescence intensity in the nuclei, whereas DHT-pretreated cells exhibited markedly reduced apoptosis (Fig. 1F).

These findings suggested that DHT mitigates cisplatin-induced cytotoxicity by reducing oxidative stress and inhibiting apoptosis in renal tubular epithelial cells. Mechanistic evidence through competitive binding further indicates the potential protective effects of DHT targeting specific protein pathways.

3.2 TRIM28 was identified as the direct molecular target of DHT via chemical proteomics and structural analysis

Next, following the competitive ABPP workflow illustrated in Fig. 2A, the protein samples obtained from the labeling of DHT-treated cells were processed and subsequently analyzed by LC-MS/MS. A relatively high proportion of cysteine-containing peptides was observed in the control and DHT-treated groups, indicating that DHT effectively competes for binding to cysteine residues with the desulfurized biotin IAA-probe at the proteomic level. This finding was consistent with the fluorescent gel results. The LC-MS/MS results highlighted that TRIM28 (Cys232) exhibited the strongest competitive binding effect upon DHT treatment (Fig. 2B, C).

To confirm TRIM28 as the covalent target of DHT, we performed multiple validation experiments. Firstly, immunofluorescence staining demonstrated that DHT effectively competed with the IAA-probe and exhibited

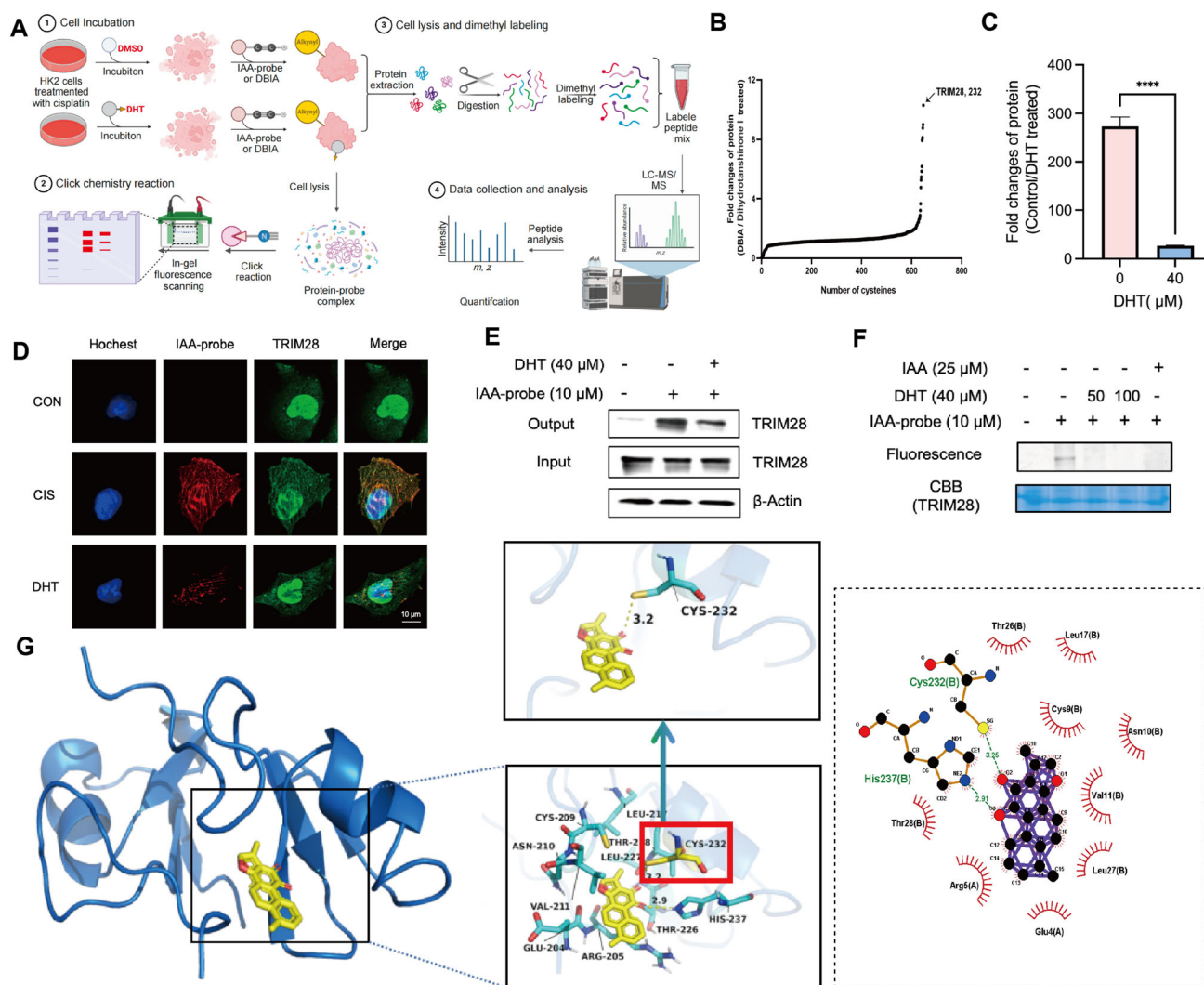


Fig. 2 Identification and validation of DHT targets using ABPP. **A** Activity-based protein profiling (ABPP) workflow for identifying the molecular target of dihydrotanshinone I (DHT) in the cisplatin-induced HK2 cell injury model. **B** Identification of TRIM28 as a potential protein target of DHT in HK2 via ABPP. **C** Competitive effect of DHT on TRIM28 binding to the iodoacetamide (IAA)-probe. **D** DHT markedly diminishes the colocalization of TRIM28 (green) with the IAA-probe (red) via immunofluorescence in HK2 cells. Control cells were treated with DMSO for 4 h, and the experimental groups were treated with 10 μ M cisplatin and 40 μ M DHT for 4 h. **E** Interaction of DHT with TRIM28 in HK2 cells via pull-down assays. **F** Competitive binding of DHT and IAA-alkyne probe to the purified recombinant TRIM28 protein in in-gel fluorescence assays. **G** Molecular docking analysis of DHT with TRIM28 reveals its potential binding sites, including the key residue CYS-232. **** $p < 0.0001$

subcellular colocalization with TRIM28 (Fig. 2D). Thereafter, pull-down assays revealed that DHT significantly reduced TRIM28 protein abundance in the competition group compared with the control (Fig. 2E). Similar results were observed when the purified recombinant TRIM28 protein was used (Fig. 2F), thereby eliminating potential confounding effects from cellular complexity.

To further delineate the binding mode, molecular docking predicted that DHT (yellow) occupies a cavity within TRIM28 (blue), forming stable interactions with the key residues (Fig. 2G). The magnified view highlights Cys232 as the central binding site, where DHT engages in

covalent interactions. Additional residues, including Cys209, Leu217, Thr228, and Val211, likely stabilize this binding through hydrogen bonding and hydrophobic forces. Together, these results unequivocally establish TRIM28 as the direct covalent target of DHT.

3.3 Quantitative proteomic analysis of DHT effects on cisplatin-induced proteome changes in HK2 cells

Proteomic profiling was performed to elucidate the molecular mechanisms underlying the protective effects of

DHT against cisplatin-induced cytotoxicity in HK2 cells. The workflow for the proteomics experiment is summarized in Fig. 3A, and volcano-plot analysis revealed a substantial number of differentially expressed proteins (DEPs) induced by cisplatin (240 downregulated, 85 upregulated proteins; Fig. 3B, left). However, DHT treatment restored the protein expression levels (195 upregulated, 58 downregulated proteins) compared with cisplatin alone (Fig. 3B, right). Among the identified DEPs, proteins such as HBD, PTGES, ENPEP, IL18, and FAM83D exhibited significant alterations. DHT treatment reversed the cisplatin-induced dysregulation of these proteins (Fig. 3C), demonstrating a restorative effect on the proteomic profile.

To further reveal the protein expression trends, DEPs were categorized into four distinct clusters based on hierarchical clustering (Fig. 3D). Cluster 2 shows proteins upregulated by cisplatin and downregulated following DHT treatment, whereas Cluster 3 demonstrates the opposite pattern. These clusters provide insights into the protein groups that are responsive to cellular injury and DHT intervention. KEGG pathway enrichment analysis identified critical pathways affected by cisplatin, including “reactive oxygen species,” “apoptosis,” and “autophagy,” all of which were significantly resolved by DHT treatment (Fig. 3E, left). Similarly,

GO-enrichment analysis highlighted biological processes, including “apoptosis,” “DNA repair,” “cell cycle regulation,” and “protein folding,” as the key pathways modulated by DHT treatment (Fig. 3E, right).

These results demonstrated that DHT effectively modulated the expression of cisplatin-altered proteins associated with oxidative stress and apoptosis. Proteomics profiling and functional enrichment analysis suggested that DHT rescued cellular damage by regulating pathways, such as ROS balance, autophagy, and apoptosis, thereby establishing its protective roles in cisplatin-induced injury, which align with previous results.

3.4 DHT reduces cisplatin-induced ROS accumulation and apoptosis via antioxidant and antiapoptotic mechanisms

To elucidate the mechanisms by which DHT mitigates cisplatin-induced cytotoxicity, we assessed its effects on intracellular ROS accumulation levels and apoptosis in HK2 cells. Fluorescence microscopy with DCFH-DA staining revealed a marked increase in ROS accumulation upon cisplatin treatment compared with the control group. DHT (100 μ M) and the positive antioxidant control NAC

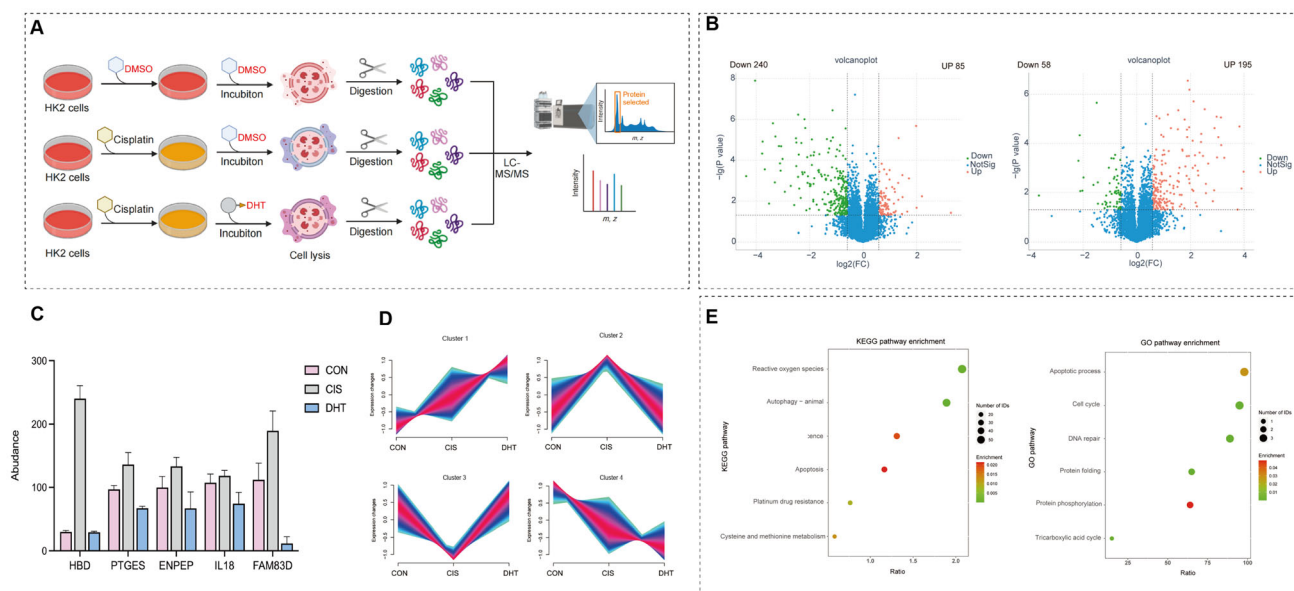


Fig. 3 Effects on protein expression in potentially relevant pathways. **A** Schematic workflow of the proteomics experiment. HK2 cells were treated with DMSO (control), cisplatin (CIS, 10 μ M), or cisplatin and dihydrotanshinone I (DHT, 100 μ M) together for 24 h. After cell lysis, protein digestion, and LC-MS/MS analysis, the proteomic profiles were quantified and compared. **B** Volcano plots illustrate the differentially expressed proteins (DEPs) in two pairwise comparisons: CIS versus CON (left panel) and DHT + CIS versus CIS (right panel). Upregulated proteins are denoted by red dots; downregulated proteins are marked by green dots (threshold lines: $\log_2(\text{FC}) > 1.5$, $p < 0.05$). **C** Protein abundance of HBD, PTGES, ENPEP, IL18, and FAM83D across the different treatment conditions (CON, CIS, and DHT), as measured by proteomics analysis. **D** Cluster analysis of DEPs identified four main response patterns (Cluster 1–4). **E** KEGG and GO pathway enrichment analysis of the DEPs. Bubble size represents the number of enriched DEPs, and color intensity indicates the enrichment significance.

(2 mM) significantly reduced ROS generation, as evidenced by diminished green fluorescence intensity (Fig. 4A). CCK-8 assays confirmed the protective effects of DHT on cell viability in cisplatin-treated HK2 cells, which revealed that cisplatin significantly reduced the cell viability compared with the control group, whereas DHT restored cell viability in a dose-dependent manner (Fig. 4B). NAC also improved cell viability, suggesting that DHT may exert its protective effects through its antioxidant properties.

To investigate DHT's antiapoptotic potential, the pan-caspase inhibitor Z-VAD-FMK was employed. Similar to DHT, Z-VAD-FMK significantly enhanced cell viability in the cisplatin-treated HK2 cells (Fig. 4C), indicating the involvement of apoptosis suppression in DHT-mediated protection. Flow cytometry with Annexin V-FITC/PI staining further demonstrated the reduction of cisplatin-induced apoptosis by DHT pretreatment (Fig. 4D). Cisplatin-induced high cell death rates were significantly reduced by DHT pretreatment.

3.5 DHT reduces cisplatin-induced ROS accumulation and apoptosis via antioxidant and antiapoptotic mechanisms

These experiments revealed that DHT can alleviate renal tubular epithelial cell damage induced by cisplatin in vitro. The following experiments demonstrated DHT's protective effect on cisplatin-induced nephrotoxicity in vitro. Male C57BL/6 mice were pretreated with DHT ($15 \text{ mg kg}^{-1} \text{ day}^{-1}$, oral gavage) for 7 days before cisplatin administration (Fig. 5A). Body weight and renal function markers were measured 72 h after cisplatin administration. Cisplatin treatment caused significant weight loss (CON: $22.9 \pm 0.3 \text{ g}$ vs. CIS: $18.3 \pm 0.2 \text{ g}$; **** $p < 0.0001$), elevated serum CREA levels (CON: $18.2 \pm 1.1 \mu\text{mol L}^{-1}$ vs. CIS: $141.2 \pm 17.9 \mu\text{mol L}^{-1}$; **** $p < 0.0001$), and increased BUN levels (CON: $7.4 \pm 0.3 \text{ mmol L}^{-1}$ vs. CIS: $65.9 \pm 14.6 \text{ mmol L}^{-1}$; **** $p < 0.0001$). However, DHT pretreatment significantly attenuated these adverse effects (Fig. 5B), demonstrating its renoprotective potential.

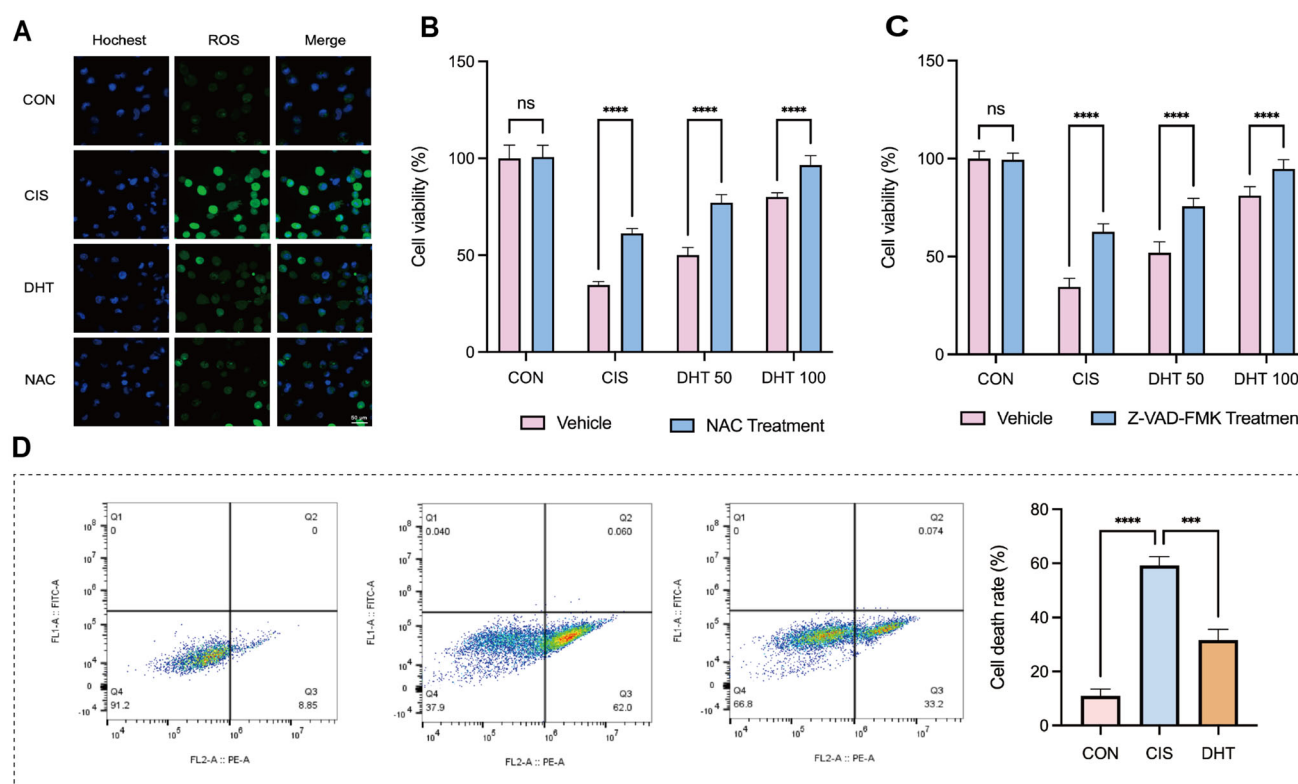


Fig. 4 In vitro validation, DHT reduced ROS and cell apoptosis. **A** Immunofluorescence images show ROS accumulation in HK2 cells stained with DCFH-DA (green) under different treatments: control (CON), cisplatin (CIS, 10 μM), cisplatin + dihydrotanshinone I (DHT, 100 μM), or cisplatin + NAC (2 mM). Nuclei were counterstained with Hoechst (blue). **B** CCK-8 assay revealed that the ROS scavenger NAC reversed cisplatin-induced HK2 cell death and DHT enhanced this effect in a dose-dependent manner. **C** Cell viability was measured via CCK-8 in HK2 cells treated with the vehicle or the apoptosis inhibitor Z-VAD-FMK in combination with the control, cisplatin, or cisplatin + DHT (50 and 100 μM). **D** Flow cytometry showing Annexin V-FITC/PI staining for apoptosis in cisplatin-treated HK2 cells with or without DHT pretreatment. Quantification of the cell death rates is shown in the right panel. *** $p < 0.001$, **** $p < 0.0001$

Histopathological analysis of kidney sections stained with H&E revealed severe tubular damage in the CIS group, characterized by tubular necrosis, cast formation, and brush border loss (Fig. 5C). Tubular injury scores were significantly elevated in the CIS group (4.4 ± 0.2 vs. 0 in CON; $****p < 0.0001$), which were ameliorated by DHT pretreatment (1.8 ± 0.4 , $***p < 0.001$ vs. CIS).

To verify whether this mechanism was related to oxidative stress and apoptosis, western blot and ELISA assays using mouse kidney tissue were performed. Western blot analysis demonstrated that apoptosis and kidney injury markers were upregulated, including cleaved caspase 3, BAX, KIM-1, and NGAL, in cisplatin-treated mice, whereas the antiapoptotic Bcl-2 levels were downregulated (Fig. 5D). DHT intervention significantly reversed these changes, indicating that its renoprotection properties function via antiapoptotic mechanisms. Furthermore, DHT reduced the oxidative stress in the renal tissues. Cisplatin administration markedly decreased the SOD activity (CON: 308.5 ± 8.8 U mg^{-1} vs. CIS: 178.8 ± 24 U mg^{-1} ; $***p < 0.001$) and increased MDA levels (CON:

1.72 ± 0.19 nmol mg^{-1} vs. CIS: 2.98 ± 0.32 nmol mg^{-1} ; $***p < 0.001$) and ROS accumulation (CON: 150.8 ± 13.9 IU mL^{-1} vs. CIS: 277.4 ± 22.6 IU mL^{-1} ; $***p < 0.001$). DHT pretreatment restored the SOD activity (252.2 ± 12.2 U mg^{-1} , $**p < 0.01$ vs. CIS) and reduced the MDA (2.11 ± 0.18 nmol mg^{-1} , $**p < 0.01$ vs. CIS) and ROS levels (180.6 ± 10.2 IU mL^{-1} , $***p < 0.001$ vs. CIS) (Fig. 5E). These findings indicate that DHT mitigates cisplatin-induced renal injury in mice by reducing oxidative stress and suppressing apoptosis.

The nephrotoxicity of cisplatin represents a substantial clinical challenge that limits the therapeutic potential of this chemotherapeutic agent [6–8]. Our study provides compelling evidence that DHT, a bioactive compound derived from *S. miltiorrhiza*, effectively mitigates cisplatin-induced AKI through a novel mechanism involving the direct targeting of TRIM28, an E3 ubiquitin ligase. This work significantly advances our understanding of natural compound-based nephroprotection by employing cutting-edge chemical proteomics approaches combined with comprehensive in vitro and in vivo validation. While

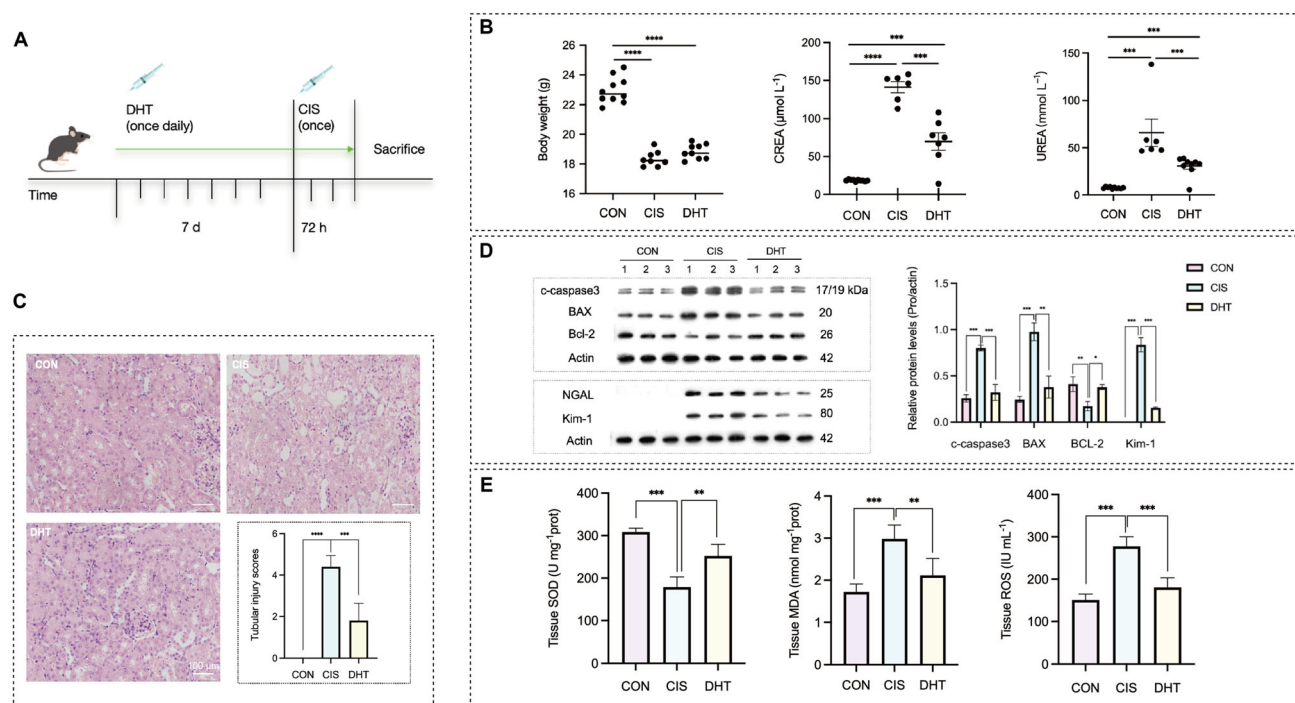


Fig. 5 DHT protecting the kidney in vivo by reducing ROS accumulation and apoptosis. **A** Experimental design for the animal model. Male mice were pretreated with 15 mg kg^{-1} dihydrotanshinone I (DHT) once daily for 7 days. On the eighth day, the mice were given a single dose of cisplatin (20 mg kg^{-1}) intraperitoneally to induce acute kidney injury. The mice were killed 72 h later for sample collection and analysis. **B** Body weight and renal function markers (CREA and BUN) measured in the control (CON), cisplatin (CIS), and DHT-pretreated groups (DHT). **C** H&E-stained images showing renal tubular injury in the three groups; quantification of the tubular injury scores is shown in the lower panel. **D** Western blot analysis of apoptosis and kidney injury markers (cleaved caspase 3, BAX, Bcl-2, KIM-1 and NGAL), with β -actin as the internal control. Quantification of the relative protein levels is shown in the right panel. **E** Key oxidative stress markers in renal tissues were tested by ELISA: SOD activity (U mg^{-1} protein), MDA levels (nmol mg^{-1} protein), and ROS (IU mL^{-1}). Data are expressed as the mean \pm standard error of the mean (SEM). $**p < 0.01$, $***p < 0.001$, $****p < 0.0001$; $n = 6$

previous studies have explored the protective effects of *S. miltiorrhiza* and its components against cisplatin nephrotoxicity, our work provides unprecedented mechanistic insights. Yuan et al. demonstrated the anti-inflammatory activity of DHT using in vivo and in vitro models, elucidating its molecular mechanism, and highlighting the involvement of the TLR4-MyD88-NF- κ B/MAPK signaling pathways [38]. However, their study did not explore DHT's antioxidant and antiapoptotic properties. Furthermore, in vitro experiments lacked a specific focus on renal tubular epithelial cells, which were essential for understanding their potential nephroprotective effects. Cao et al. showed that *S. miltiorrhiza* protects against cisplatin-induced kidney injury via nuclear factor erythroid 2-related factor 2 (NRF2) pathway upregulation, but did not identify the specific active compounds or their direct molecular targets [39]. The research relied solely on basic phenotypic analysis without employing advanced techniques, such as omics, to validate the mechanisms. Moreover, the specific protein targets through which *S. miltiorrhiza* exerts its protective effects remained unidentified. Our work addressed these limitations by using ABPP to identify TRIM28 as a key covalent binding target of DHT in renal tubular epithelial cells. Through omics analyses combined with in vitro and in vivo validation, we confirmed DHT's dual protective mechanisms via antioxidant and antiapoptotic pathways.

Our study uniquely identifies TRIM28 as the first reported covalent binding target of DHT using ABPP, a powerful chemical proteomics approach that enables unbiased target identification. This methodology represents a significant advancement over traditional pharmacological screening methods, as it directly captures drug-protein interactions in living cells. The identification of TRIM28 as DHT's target is significant given the limited understanding of TRIM28's role in renal diseases, particularly AKI, with most previous research focusing on its involvement in malignant tumors [40].

Excessive ROS accumulation represents a critical pathophysiological mechanism in the initiation and progression of AKI [12, 13]. Differential expression and functional enrichment analyses revealed multiple proteins and pathways reversed by DHT pretreatment, including those associated with ROS generation, apoptosis regulation, autophagy, and DNA repair. Critically, proteins such as HBD, PTGES, ENPEP, and IL18 were identified as key mediators that were dysregulated by cisplatin and subsequently restored following DHT treatment. These results support recent findings that emphasized the therapeutic potential of natural products targeting multipathway dysregulation in cisplatin toxicity [23, 26]. The in vivo efficacy of DHT is particularly noteworthy, as it significantly preserved the renal function and structure in cisplatin-

treated mice. The reduced tubular injury scores, decreased expression of kidney injury markers (KIM-1), and serum CREA and BUN levels collectively demonstrate the translational potential of this natural compound. Numerous studies have explored improvements to enhance cisplatin's antitumor effects from various perspectives [41]. Our research provides a new therapeutic approach by focusing on reducing cisplatin-induced nephrotoxicity through the active components of traditional Chinese medicine.

This study has a few limitations that require further consideration. First, as a key target in the mechanism of DHT's effects, the role of TRIM28 has not been fully clarified and needs to be validated further using conditional gene knockout models, and it is an important way to clarify the regulatory relationship of its upstream and downstream signaling pathways and key node molecules. Second, the in vivo efficacy of DHT is particularly noteworthy, as oral administration at 15 mg kg⁻¹ day⁻¹ significantly preserved the renal function, reduced the tubular injury scores, and restored the oxidative balance in cisplatin-treated mice. These results, combined with DHT's established safety profile in traditional medicine applications, suggest strong translational potential. However, the pharmacokinetic characteristics of DHT combined with cisplatin have not been fully explored. Future studies in this area will include a detailed pharmacokinetic analysis of the combined use of DHT and cisplatin, covering absorption, distribution, metabolism, and excretion. Additionally, we will evaluate the impact of DHT on the antitumor efficacy of cisplatin to ensure that renal protection does not compromise therapeutic outcomes in tumor models. Based on pharmacokinetic parameters, we will also work to optimize dosing regimens to maximize renal protection while minimizing potential adverse effects. In the future, combining DHT with other renoprotective agents, such as NAC, may yield synergistic effects to further reduce cisplatin-induced kidney damage. Moreover, modifying DHT's structure or creating nano-delivery systems could improve its absorption efficiency and increase its targeting of specific tissues, particularly enhancing its distribution in the kidney.

4 Conclusion

In summary, this study identifies DHT, a natural product derived from *S. miltiorrhiza*, as a promising candidate to mitigate cisplatin-induced AKI, a major side effect that limits the clinical application of platinum-based chemotherapeutics. By covalently targeting TRIM28, DHT effectively reduces ROS levels and inhibits apoptosis in the renal tubular cells, as demonstrated by in vitro studies and proteomic analyses. In the in vivo experiments using cisplatin-treated mice, DHT pretreatment significantly

preserved renal function, attenuated tubular injury, and restored the oxidative balance, thereby highlighting DHT's strong renoprotective effects. These findings establish TRIM28 as a novel drug target for oxidative damage and emphasize DHT's potential as an adjunctive therapeutic agent to improve the safety of platinum-based chemotherapy. This work bridges traditional medicinal applications with modern molecular approaches to provide new insights into the use of natural compounds as adjunctive therapies in platinum-based chemotherapy. Moreover, it establishes a foundation for further research on pharmacokinetics, formulation optimization, and combination therapy strategies, thus advancing the field of precision medicine.

Acknowledgements This work was financially supported by the National Natural Science Foundation of China (Nos. 82100709, 82200752 and 82100719) and China Postdoctoral Science Foundation (No. 2023M741797).

Author contributions Ping-Ping Sun designed the research, conducted the experiments and drafted the manuscript. Jun-Yong Sun performed the omics data analysis. Ze-Hua Li was responsible for image processing. Jing Chang and Mei-Ling Jin provided critical suggestions for improving the study. Jia-Yu Song contributed to project design and manuscript revision. Qian-Mei Sun and Xiao-Juan Wang supervised and guided the study.

Data availability The data that support the findings of this study are available from the corresponding author upon reasonable request.

Declarations

Conflict of interests The authors declare that they have no conflict of interest.

References

- [1] Ghosh S. Cisplatin: the first metal based anticancer drug. *Bioorg Chem.* 2019;88:102925. <https://doi.org/10.1016/j.bioorg.2019.102925>.
- [2] Minerva, Bhat A, Verma S, Chander G, Jamwal RS, Sharma B, Bhat A, Katyal T, Kumar R, Shah R. Cisplatin-based combination therapy for cancer. *J Cancer Res Ther.* 2023;19(3):530–536. https://doi.org/10.4103/jcrt.jcrt_792_22.
- [3] Dasari S, Tchounwou PB. Cisplatin in cancer therapy: molecular mechanisms of action. *Eur J Pharmacol.* 2014;740:364–78. <https://doi.org/10.1016/j.ejphar.2014.07.025>.
- [4] Qi L, Luo Q, Zhang Y, Jia F, Zhao Y, Wang F. Advances in toxicological research of the anticancer drug Cisplatin. *Chem Res Toxicol.* 2019;32(8):1469–86. <https://doi.org/10.1021/acs.chemrestox.9b00204>.
- [5] Zhang J, Ye ZW, Tew KD, Townsend DM. Cisplatin chemotherapy and renal function. *Adv Cancer Res.* 2021;152:305–27. <https://doi.org/10.1016/bs.acr.2021.03.008>.
- [6] Tang C, Livingston MJ, Safirstein R, Dong Z. Cisplatin nephrotoxicity: new insights and therapeutic implications. *Nat Rev Nephrol.* 2023;19(1):53–72. <https://doi.org/10.1038/s41581-022-00631-7>.
- [7] Manohar S, Leung N. Cisplatin nephrotoxicity: a review of the literature. *J Nephrol.* 2018;31(1):15–25. <https://doi.org/10.1007/s40620-017-0392-z>.
- [8] Pabla N, Dong Z. Cisplatin nephrotoxicity: mechanisms and renoprotective strategies. *Kidney Int.* 2008. <https://doi.org/10.1038/sj.ki.5002786>.
- [9] Ozkok A, Edelstein CL. Pathophysiology of cisplatin-induced acute kidney injury. *Biomed Res Int.* 2014;2014:967826. <https://doi.org/10.1155/2014/967826>.
- [10] Holditch SJ, Brown CN, Lombardi AM, Nguyen KN, Edelstein CL. Recent advances in models, mechanisms, biomarkers, and interventions in Cisplatin-induced acute kidney injury. *Int J Mol Sci.* 2019. <https://doi.org/10.3390/ijms20123011>.
- [11] McSweeney KR, Gadanec LK, Qaradakh T, Ali BA, Zulli A, Apostolopoulos V. Mechanisms of cisplatin-induced acute kidney injury: pathological mechanisms, pharmacological interventions, and genetic mitigations. *Cancers (Basel).* 2021. <https://doi.org/10.3390/cancers13071572>.
- [12] Mirzaei S, Hushmandi K, Zabolian A, Saleki H, Torabi SMR, Ranjbar A, SeyedSaleh S, Sharifzadeh SO, Khan H, Ashrafzadeh M, Zarrabi A, Ahn K-S. Elucidating role of reactive oxygen species (ROS) in cisplatin chemotherapy: a focus on molecular pathways and possible therapeutic strategies. *Molecules.* 2021. <https://doi.org/10.3390/molecules26082382>.
- [13] García MMS, Acquier A, Suarez G, Gomez NV, Gorostizaga A, Mendez CF, Paz C. Cisplatin inhibits testosterone synthesis by a mechanism that includes the action of reactive oxygen species (ROS) at the level of P450_{sc}. *Chem Biol Interact.* 2012;199(3):185–91. <https://doi.org/10.1016/j.cbi.2012.08.012>.
- [14] Mirzaei S, Mohammadi AT, Gholami MH, Hashemi F, Zarrabi A, Zabolian A, Hushmandi K, Makvandi P, Samec M, Liskova A, Kubatka P, Nabavi N, Aref AR, Ashrafzadeh M, Khan H, Najafi M. Nrf2 signaling pathway in cisplatin chemotherapy: potential involvement in organ protection and chemoresistance. *Pharmacol Res.* 2021;167:105575. <https://doi.org/10.1016/j.phrs.2021.105575>.
- [15] Zhang S, Liu Q, Chang M, Pan Y, Yahaya BH, Liu Y, Lin J. Chemotherapy impairs ovarian function through excessive ROS-induced ferroptosis. *Cell Death Dis.* 2023;14(5):340. <https://doi.org/10.1038/s41419-023-05859-0>.
- [16] Morgan KP, Buie LW, Savage SW. The role of mannitol as a nephroprotectant in patients receiving cisplatin therapy. *Ann Pharmacother.* 2012;46(2):276–81. <https://doi.org/10.1345/aph.1Q333>.
- [17] Eltamany EE, Elhady SS, Nafie MS, Ahmed HA, Abo-Elmatty DM, Ahmed SA, Badr JM, Abdel-Hamed AR. The antioxidant *Carrichtera annua* DC. ethanolic extract counteracts cisplatin triggered hepatic and renal toxicities. *Antioxidants (Basel).* 2021. <https://doi.org/10.3390/antiox10060825>.
- [18] Abdel-Wahab WM, Moussa FI, Saad NA. Synergistic protective effect of N-acetylcysteine and taurine against cisplatin-induced nephrotoxicity in rats. *Drug Des Devel Ther.* 2017;11:901–8. <https://doi.org/10.2147/DDDT.S131316>.
- [19] Nisar S, Feinfeld DA. N-acetylcysteine as salvage therapy in cisplatin nephrotoxicity. *Ren Fail.* 2002;24(4):529–33. <https://doi.org/10.1081/JDI-120006780>.
- [20] Sancho-Martínez SM, Prieto-García L, Prieto M, Fuentes-Calvo I, López-Novoa JM, Morales AI, Martínez-Salgado C, López-Hernández FJ. N-acetylcysteine transforms necrosis into apoptosis and affords tailored protection from cisplatin cytotoxicity. *Toxicol Appl Pharmacol.* 2018;349:83–93. <https://doi.org/10.1016/j.taap.2018.04.010>.
- [21] Mashayekhi-Sardoo H, Rezaee R, Yarmohammadi F, Karimi G. Targeting endoplasmic reticulum stress by natural and chemical compounds ameliorates Cisplatin-induced nephrotoxicity: a

- review. *Biol Trace Elem Res.* 2024. <https://doi.org/10.1007/s12011-024-04351-w>.
- [22] Lin SY, Chang CL, Liou KT, Kao YK, Wang YH, Chang CC, Kuo TBJ, Huang HT, Yang CCH, Liaw CC, Shen YC. The protective role of *Achyranthes aspera* extract against cisplatin-induced nephrotoxicity by alleviating oxidative stress, inflammation, and PANoptosis. *J Ethnopharmacol.* 2024;319(Pt 1):117097. <https://doi.org/10.1016/j.jep.2023.117097>.
- [23] Jin F, Chen X, Yan H, Xu Z, Yang B, Luo P, He Q. Bisdemethoxycurcumin attenuates cisplatin-induced renal injury through anti-apoptosis, anti-oxidant and anti-inflammatory. *Eur J Pharmacol.* 2020;874:173026. <https://doi.org/10.1016/j.ejphar.2020.173026>.
- [24] Jung K, An JM, Eom DW, Kang KS, Kim SN. Preventive effect of fermented black ginseng against cisplatin-induced nephrotoxicity in rats. *J Ginseng Res.* 2017;41(2):188–94. <https://doi.org/10.1016/j.jgr.2016.03.001>.
- [25] Xie X, Wu F, Tian J, Liu Z, He H, Bao D, Li G, Li H, Chen J, Lai Y, Chen Z, Fan J, Chen G, Lai C. Pyrocatechol alleviates cisplatin-induced acute kidney injury by inhibiting ROS production. *Oxid Med Cell Longev.* 2022;2022:2158644. <https://doi.org/10.1155/2022/2158644>.
- [26] Fang CY, Lou DY, Zhou LQ, Wang JC, Yang B, He QJ, Wang JJ, Weng QJ. Natural products: potential treatments for cisplatin-induced nephrotoxicity. *Acta Pharmacol Sin.* 2021;42(12):1951–69. <https://doi.org/10.1038/s41401-021-00620-9>.
- [27] Ridzuan NRA, Rashid NA, Othman F, Budin SB, Hussan F, Teoh SL. Protective role of natural products in Cisplatin-induced nephrotoxicity. *Mini Rev Med Chem.* 2019;19(14):1134–43. <https://doi.org/10.2174/1389557519666190320124438>.
- [28] Sun C, Han B, Zhai Y, Zhao H, Li X, Qian J, Hao X, Liu Q, Shen J, Kai G. Dihydrotanshinone I inhibits ovarian tumor growth by activating oxidative stress through Keap1-mediated Nrf2 ubiquitination degradation. *Free Radic Biol Med.* 2022;180:220–35. <https://doi.org/10.1016/j.freeradbiomed.2022.01.015>.
- [29] Li Z, Mo RL, Gong JF, Han L, Wang WF, Huang DK, Xu JG, Sun YJ, Chen S, Han GC, Sun DQ. Dihydrotanshinone I inhibits gallbladder cancer growth by targeting the Keap1-Nrf2 signaling pathway and Nrf2 phosphorylation. *Phytomedicine.* 2024;129:155661. <https://doi.org/10.1016/j.phymed.2024.155661>.
- [30] Wei Z, Zhan X, Ding K, Xu G, Shi W, Ren L, Fang Z, Liu T, Hou X, Zhao J, Li H, Li J, Li Z, Li Q, Lin L, Yang Y, Xiao X, Bai Z, Cao J. Dihydrotanshinone I specifically inhibits NLRP3 inflammasome activation and protects against septic shock in vivo. *Front Pharmacol.* 2021;12:750815. <https://doi.org/10.3389/fphar.2021.750815>.
- [31] Yue H, Yang Z, Ou Y, Liang S, Deng W, Chen H, Zhang C, Hua L, Hu W, Sun P. Tanshinones inhibit NLRP3 inflammasome activation by alleviating mitochondrial damage to protect against septic and gouty inflammation. *Int Immunopharmacol.* 2021;97:107819. <https://doi.org/10.1016/j.intimp.2021.107819>.
- [32] Yue J, Hao D, Wang Y, Guo J, Liu S, Meng L, Liu J. The multifaceted mechanisms of Dihydrotanshinone I in the treatment of tumors. *Biomed Pharmacother.* 2024;175:116635. <https://doi.org/10.1016/j.biopha.2024.116635>.
- [33] Jiang X-L, Deng B, Deng S-H, Cai M, Ding W-J, Tan Z-B, Chen R-X, Xu Y-C, Xu H-L, Zhang S-W, Zhang S-Q, Liu B, Zhang J-Z. Dihydrotanshinone I inhibits the growth of hepatoma cells by direct inhibition of Src. *Phytomedicine.* 2022;95:153705. <https://doi.org/10.1016/j.phymed.2021.153705>.
- [34] Chen X, Yu J, Zhong B, Lu J, Lu JJ, Li S, Lu Y. Pharmacological activities of dihydrotanshinone I, a natural product from *Salvia miltiorrhiza* Bunge. *Pharmacol Res.* 2019;145:104254. <https://doi.org/10.1016/j.phrs.2019.104254>.
- [35] Wang X, Jing Z, Huang X, Liu X, Zhang Y, Wang Z, Ma P. PD-L1 antibody conjugated dihydrotanshinone I-loaded polymeric nanoparticle for targeted cancer immunotherapy combining PD-L1 blockade with immunogenic cell death. *Int J Pharm.* 2024;667(Pt B):125004. <https://doi.org/10.1016/j.ijpharm.2024.125004>.
- [36] Wang M, Xiang Y, Wang R, Zhang L, Zhang H, Chen H, Luan X, Chen L. Dihydrotanshinone I inhibits the proliferation and growth of oxaliplatin-resistant human HCT116 colorectal cancer cells. *Molecules.* 2022. <https://doi.org/10.3390/molecules27227774>.
- [37] Deng H, Lei Q, Wu Y, He Y, Li W. Activity-based protein profiling: recent advances in medicinal chemistry. *Eur J Med Chem.* 2020;191:112151. <https://doi.org/10.1016/j.ejmech.2020.112151>.
- [38] Yuan R, Huang L, Du L-J, Feng J-F, Li J, Luo Y-Y, Xu Q-M, Yang S-L, Gao H, Feng Y-L. Dihydrotanshinone exhibits an anti-inflammatory effect *in vitro* and *in vivo* through blocking TLR4 dimerization. *Pharmacol Res.* 2019;142:102–14. <https://doi.org/10.1016/j.phrs.2019.02.017>.
- [39] Cao S-S, Yan M, Hou Z-Y, Chen Y, Jiang Y-S, Fan X-R, Fang P-F, Zhang B-K. Danshen modulates Nrf2-mediated signaling pathway in cisplatin-induced renal injury. *J Huazhong Univ Sci Technolog Med Sci.* 2017;37(5):761–5. <https://doi.org/10.1007/s11596-017-1801-1>.
- [40] Czerwińska P, Mazurek S, Wiznerowicz M. The complexity of TRIM28 contribution to cancer. *J Biomed Sci.* 2017;24(1):63. <https://doi.org/10.1186/s12929-017-0374-4>.
- [41] Man X-Y, Sun Z-W, Li S-H, Xu G, Li W-J, Zhang Z-L, Liang H, Yang F. Development of a Pt(II) compound based on indocyanine green@human serum albumin nanoparticles: integrating phototherapy, chemotherapy and immunotherapy to overcome tumor cisplatin resistance. *Rare Met.* 2024;43(11):6006–22. <https://doi.org/10.1007/s12598-024-02759-w>.

Springer Nature or its licensor (e.g. a society or other partner) holds exclusive rights to this article under a publishing agreement with the author(s) or other rightsholder(s); author self-archiving of the accepted manuscript version of this article is solely governed by the terms of such publishing agreement and applicable law.